Applied Surface Science 389 (2016) 438–446

Contents lists available at ScienceDirect

Applied Surface Science

journal homepage: www.elsevier.com/locate/apsusc

Quantitative analysis of Fe and Co in Co-substituted magnetite using XPS: The application of non-linear least squares fitting (NLLSF)

Hongmei Liu[a,*], Gaoling Wei[b], Zhen Xu[c], Peng Liu[a,d], Ying Li[a,d]

[a] CAS Key Laboratory of Mineralogy and Metallogeny/Guangdong Provincial Key Laboratory of Mineral Physics and Materials, Guangzhou Institute of Geochemistry, Chinese Academy of Sciences, Guangzhou, 510640, China
[b] Guangdong Key Laboratory of Agricultural Environment Pollution Integrated Control, Guangdong Institute of Eco-Environmental and Soil Sciences, Guangzhou, 510650, China
[c] School of Materials Science and Engineering, Central South University, Changsha, 410012, China
[d] University of Chinese Academy of Sciences, Beijing, 100049, China

ARTICLE INFO

Article history:
Received 11 May 2016
Received in revised form 22 July 2016
Accepted 26 July 2016
Available online 27 July 2016

Keywords:
Non-linear least squares fitting
Quantitative analysis
X-ray photoelectron spectroscopy
Co-substituted magnetite

ABSTRACT

Quantitative analysis of Co and Fe using X-ray photoelectron spectroscopy (XPS) is of important for the evaluation of the catalytic ability of Co-substituted magnetite. However, the overlap of XPS peaks and Auger peaks for Co and Fe complicate quantification. In this study, non-linear least squares fitting (NLLSF) was used to calculate the relative Co and Fe contents of a series of synthesized Co-substituted magnetite samples with different Co doping levels. NLLSF separated the XPS peaks of Co 2p and Fe 2p from the Auger peaks of Fe and Co, respectively. Compared with a control group without fitting, the accuracy of quantification of Co and Fe was greatly improved after elimination by NLLSF of the disturbance of Auger peaks. A catalysis study confirmed that the catalytic activity of magnetite was enhanced with the increase of Co substitution. This study confirms the effectiveness and accuracy of the NLLSF method in XPS quantitative calculation of Fe and Co coexisting in a material.

1. Introduction

Extensive research has focused on transition metal (Co, V, Ni, Mn, Ti, etc.) substituted magnetite because of its surface catalytic properties [1–5]. For example, the catalytic activities of magnetite in the heterogeneous Fenton reaction are greatly improved by the introduction of Mn [6], V [7], and Co [3]. The chemical state, content, and distribution of substituting cations in the spinel structure of magnetite are key factors that strongly affected the catalytic performance of magnetite [8]. Thus, quantitative analysis of the active metal cations in the surface of magnetite is important for the evaluation of catalytic ability.

X-ray photoelectron spectroscopy (XPS) is an effective and reliable analytical method for elemental identification and quantification of the chemical states of active surface atoms because it is surface sensitive and non-destructive [9]. Most XPS studies of magnetite were focused on the determination of the Fe^{2+}/Fe^{3+} ratio [10,11] and the effects on the adsorption, reduction, or removal of heavy metals [12–14]. Few reports have examined the relative quantities of the substitution element and Fe in transition metal-substituted magnetite, providing the motivation for the present study.

The photoelectron spectrum of transition metal oxides is typically complicated due to peak asymmetries, complex multiplet splitting, shake-up and plasmon loss structures, and uncertain, overlapping energies [9,15]. For example, the Fe 2p region (700–740 eV) overlaps with the Auger peak of Co (713 eV); similarly, the Auger peak of Fe (784 eV) appears within the Co 2p region (770–815 eV) [16]. Consequently, when these two elements coexist in the same sample, the peak shapes of Fe 2p and Co 2p are quite different from their respective standard spectra. Thus, for Co-substituted magnetite, the disturbance caused by Auger peaks of Fe and Co may result in the over- or underestimation of the content of these elements when only the original 2p peaks of Fe and Co are used for quantification.

To resolve the complicated XPS spectra of transition metal oxides, extensive, detailed analyses are performed using different background-subtraction methods or curve-fitting methods [17,18]. Non-linear least squares fitting (NLLSF) is one commonly used fitting method. NLLSF is a form of least squares analysis that is used

* Corresponding author at: Engineer of CAS Key Laboratory of Mineralogy and Metallogeny/Guangdong Provincial Key Laboratory of Mineral Physics and Materials, Guangzhou Institute of Geochemistry, Chinese Academy of Sciences (CAS), Wushan, Guangzhou 510640, China.
E-mail address: hmliu@gig.ac.cn (H. Liu).

http://dx.doi.org/10.1016/j.apsusc.2016.07.146
0169-4332/

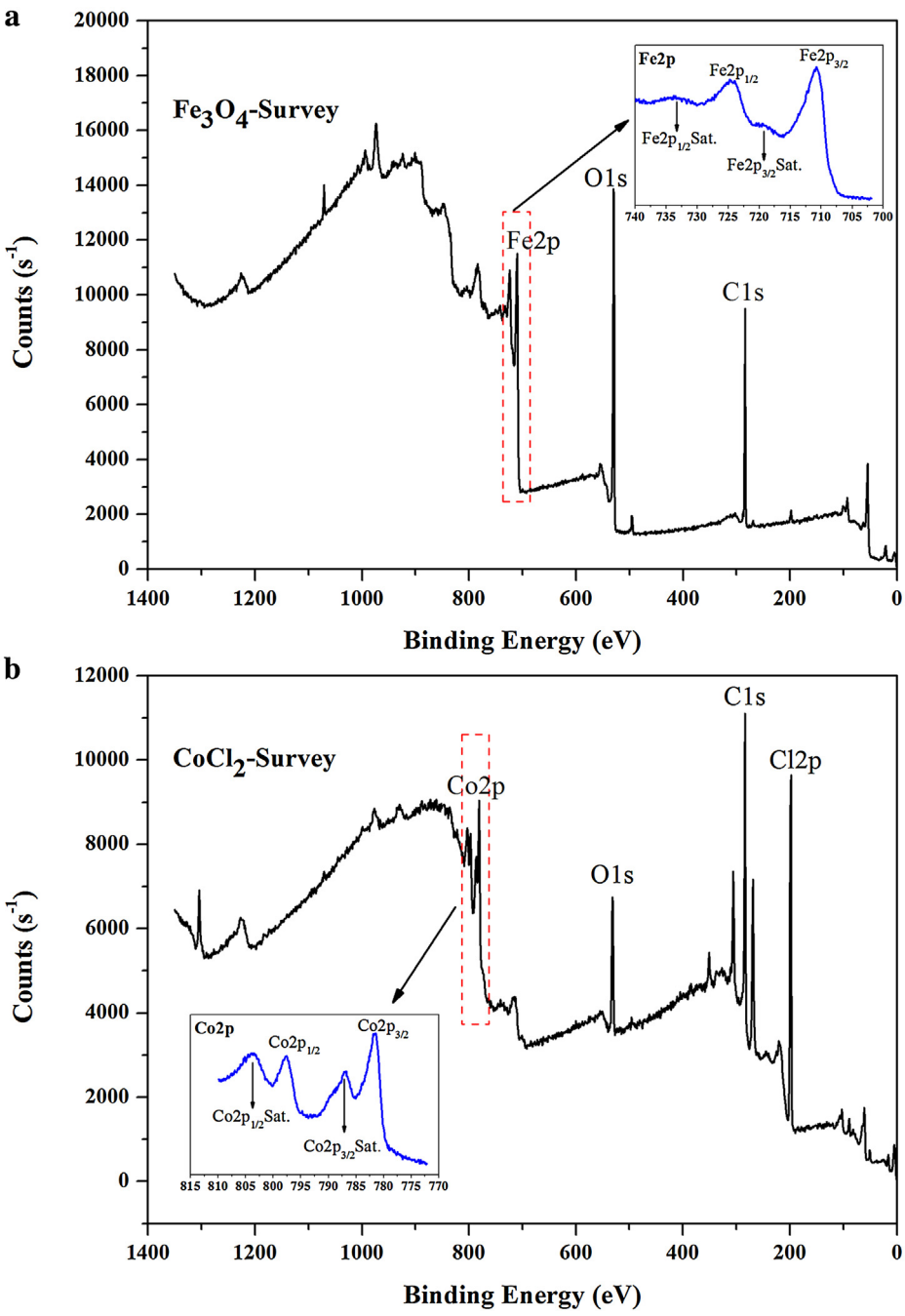

Fig. 1. XPS survey spectra of the reference samples (magnetite (a), cobalt chloride (b)).

to fit a set of m observations using a model that is non-linear in n unknown parameters ($m > n$). NLLSF is used in some forms of non-linear regression. The basis of NLLSF is to approximate the model by a linear regression and to refine the parameters by successive iterations. When using NLLSF to fit an XPS spectrum complicated by peak overlapping, references must first be defined. The reference components can be obtained from various sources, such as from within the multi-level data set, standard data (a pure component spectrum), or derived data (synthetic components obtained by peak fitting). By adjusting the shift parameters, NLLSF allows the peak intensity and peak position of reference spectra to be automatically optimised to get the best fitting result (in the form of an envelope curve) for the original data. Then, by comparison with the original data, the interference peak can be separated from the target XPS peak after fitting, and the relative content of the corresponding components can also be accurately quantified.

In this study, the NLLSF method was adopted for the quantitative analysis of the XPS spectra of a series of synthesized Co-substituted magnetite samples with different Co dopant amounts. We aimed to eliminating the disturbance caused by the Auger peaks of Co and Fe, obtain accurate quantification results for Co and Fe in Co-substituted magnetite, and consequently provide useful information for a follow-up study on the catalytic mechanism of this material.

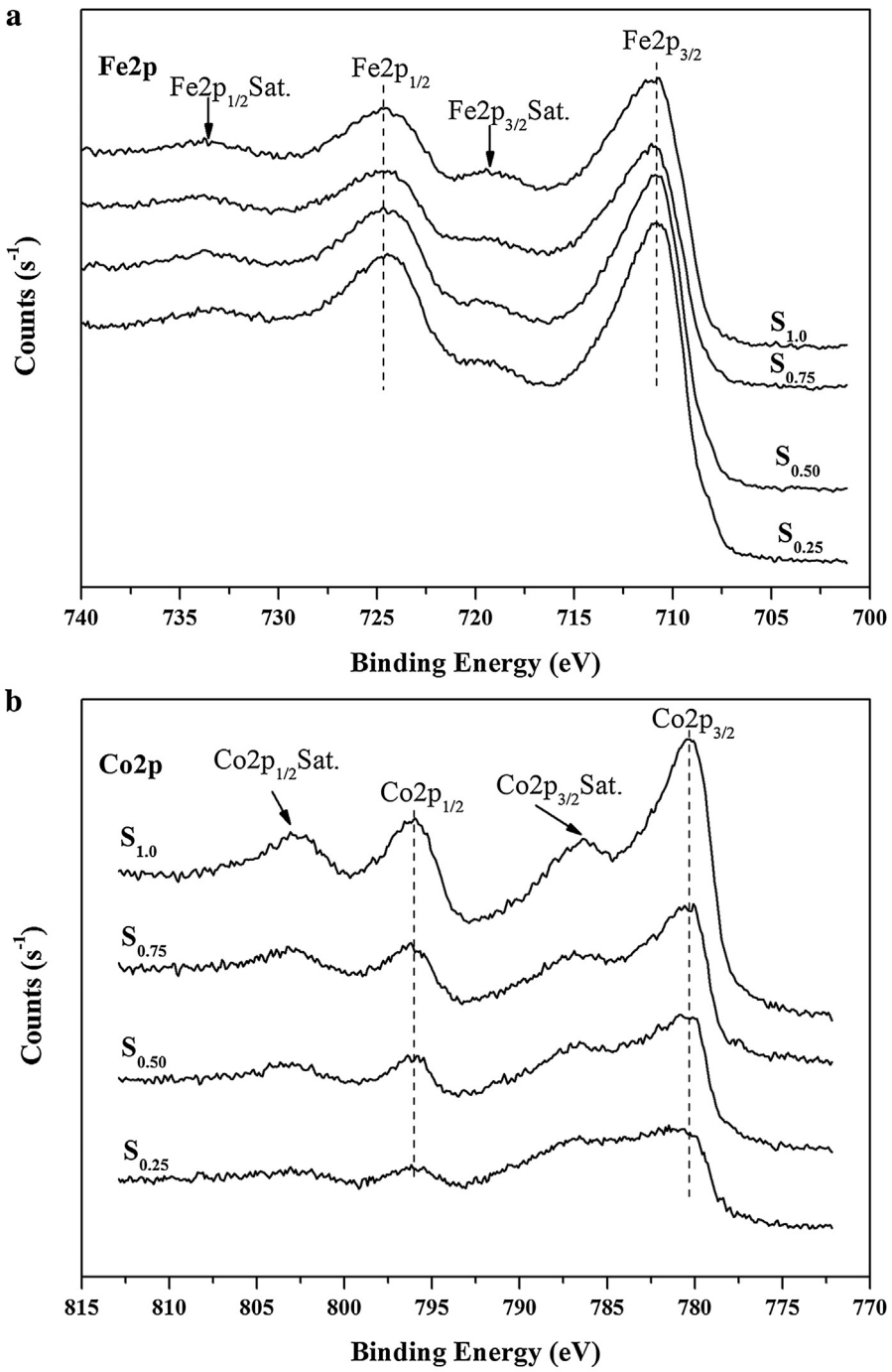

Fig. 2. Original Fe 2p and Co 2p spectra of the Co-substituted magnetite.

2. Experimental

2.1. Preparation of magnetite samples

All chemicals and reagents used in this study were of analytical grade. Co- substituted magnetite samples were synthesized using magnetite (Fe_3O_4) and cobalt chloride ($CoCl_2$) by a precipitation-oxidation routine [4,5]. The resultant samples were labeled $S_{0.25}$, $S_{0.50}$, $S_{0.75}$, and $S_{1.0}$, corresponding to the initial Co doping amounts (x) in $Fe_{3-x}Co_xO_4$ of 0.25, 0.50, 0.75, and 1.0, respectively. These values were theoretical; the actual values were determined by chemical analysis.

2.2. Characterization and methods

The chemical composition of the prepared Co-substituted magnetite samples was determined by chemical analysis. The Fe content and Fe^{2+}/Fe^{3+} ratio were measured spectrophotometrically by the phenanthroline [19,20]. The Co content and valence were detected using nitroso R salt spectrophotometric method [21] and X-ray absorption near-edge structure spectroscopy (XANES), respectively.

The X-ray diffraction (XRD) patterns of the samples were recorded between 10° and 80° at a scan rate of 1° min^{-1} using a

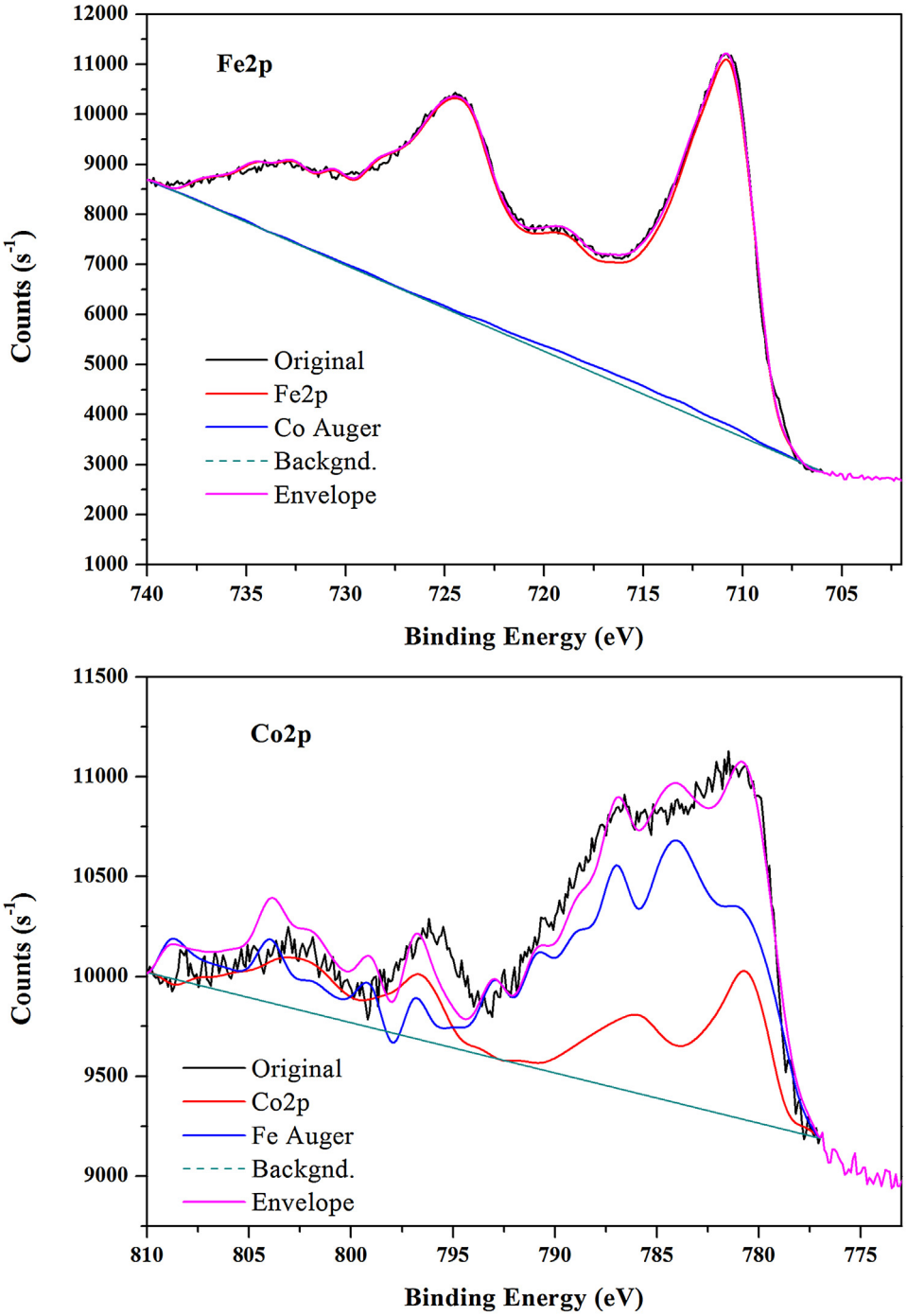

Fig. 3. NLLSF results for $S_{0.25}$.

Bruker D8 Advance diffractometer with a Ni filter and Cu Kα radiation (40 kV and 40 mA).

XPS measurements were performed using a K-Alpha X-ray photoelectron spectrometer (Thermo Fisher Scientific, UK) with a monochromatic Al Kα X-ray source (excitation energy = 1468.6 eV). The XPS analysis chamber was evacuated to ultra-high vacuum (a pressure of 5×10^{-8} mbar or lower) before analysis. Spectra were collected from 0 to 1350 eV using an X-ray spot size of 400 μm with a pass energy of 100 eV for wide scan and 30 eV for individual elements. Binding energies were corrected relative to the carbon 1 s signal at 284.8 eV.

The XPS data analysis was completed using Avantage software. The NLLSF procedure can be summarized as follows. (1) Reference spectra were defined and loaded into software, along with the original spectrum. (2) NLLSF was selected as the fitting method. (3) The linear method was chosen for background subtraction. (4) The binding energy range for background subtraction was identified. (5) Shift parameters (Max shift range, Step size) were set. (6) NLLSF was initiated. Then, by repeatedly adjusting the shift parameters, a best-fitting result was obtained. Once the fitting result was accepted, the different component spectra in the original overlapping data were isolated (the real Fe 2p and Co Auger peaks from the original Fe

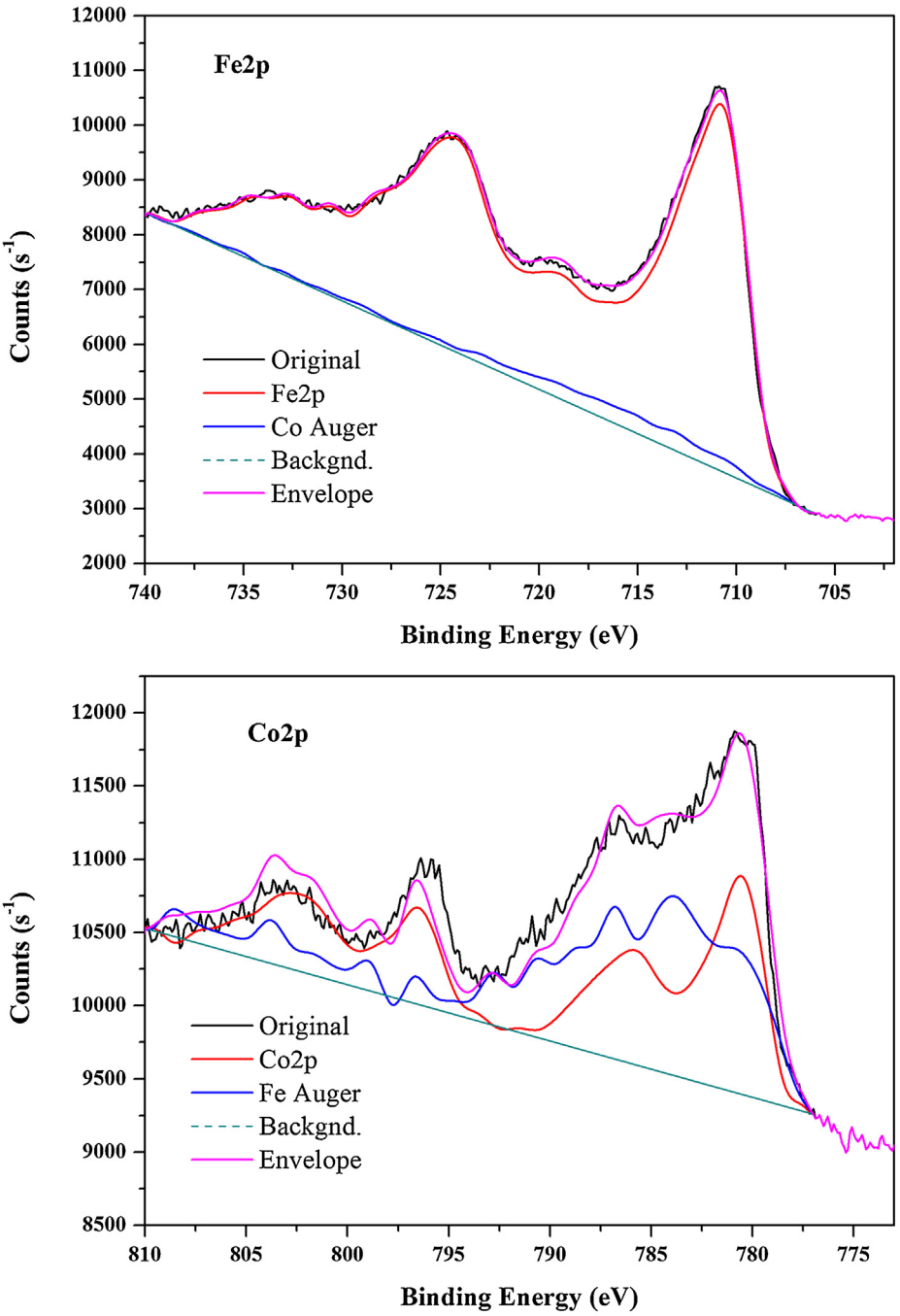

Fig. 4. NLLSF results for $S_{0.50}$.

2p region, and the real Co 2p and Fe Auger peaks from the original Co 2p region), and the corresponding atomic ratio of each element was obtained. For the comparison group, the SMART method was selected for background subtraction, and the atomic ratio of Fe to Co was directly calculated from the original Fe 2p and Co 2p peaks without curve fitting.

3. Results and discussion

3.1. Chemical analysis and XRD

From the chemical analysis results (Table 1), it can be seen that the content proportionality of cobalt to iron increases with the content increment of Co, indicating the substitution of cobalt for iron.

Table 1
Chemical analysis results for Co-substituted magnetite samples.

Sample	Co/Fe mass ratio	Fe/Co atomic ratio	Fe^{2+}/Fe^{3+} ratio	Formula
$S_{0.25}$	0.075	14.00	0.28	$Fe^{2+}_{0.61}Fe^{3+}_{2.19}Co^{2+}_{0.20}O_4$
$S_{0.50}$	0.177	5.98	0.58	$Fe^{2+}_{0.94}Fe^{3+}_{1.63}Co^{2+}_{0.43}O_4$
$S_{0.75}$	0.300	3.48	0.71	$Fe^{2+}_{0.97}Fe^{3+}_{1.36}Co^{2+}_{0.67}O_4$
$S_{1.0}$	0.452	2.33	0.75	$Fe^{2+}_{0.90}Fe^{3+}_{1.20}Co^{2+}_{0.90}O_4$

XANES results indicated the valence of Co in magnetite samples was mainly +2 (see Supplementary data, Fig. S1). The chemical formula and atomic ratio of Fe to Co of these samples as calculated from the chemical analysis results are also shown in Table 1. The atomic ratio of Fe to Co decreased with increasing of the Co doping

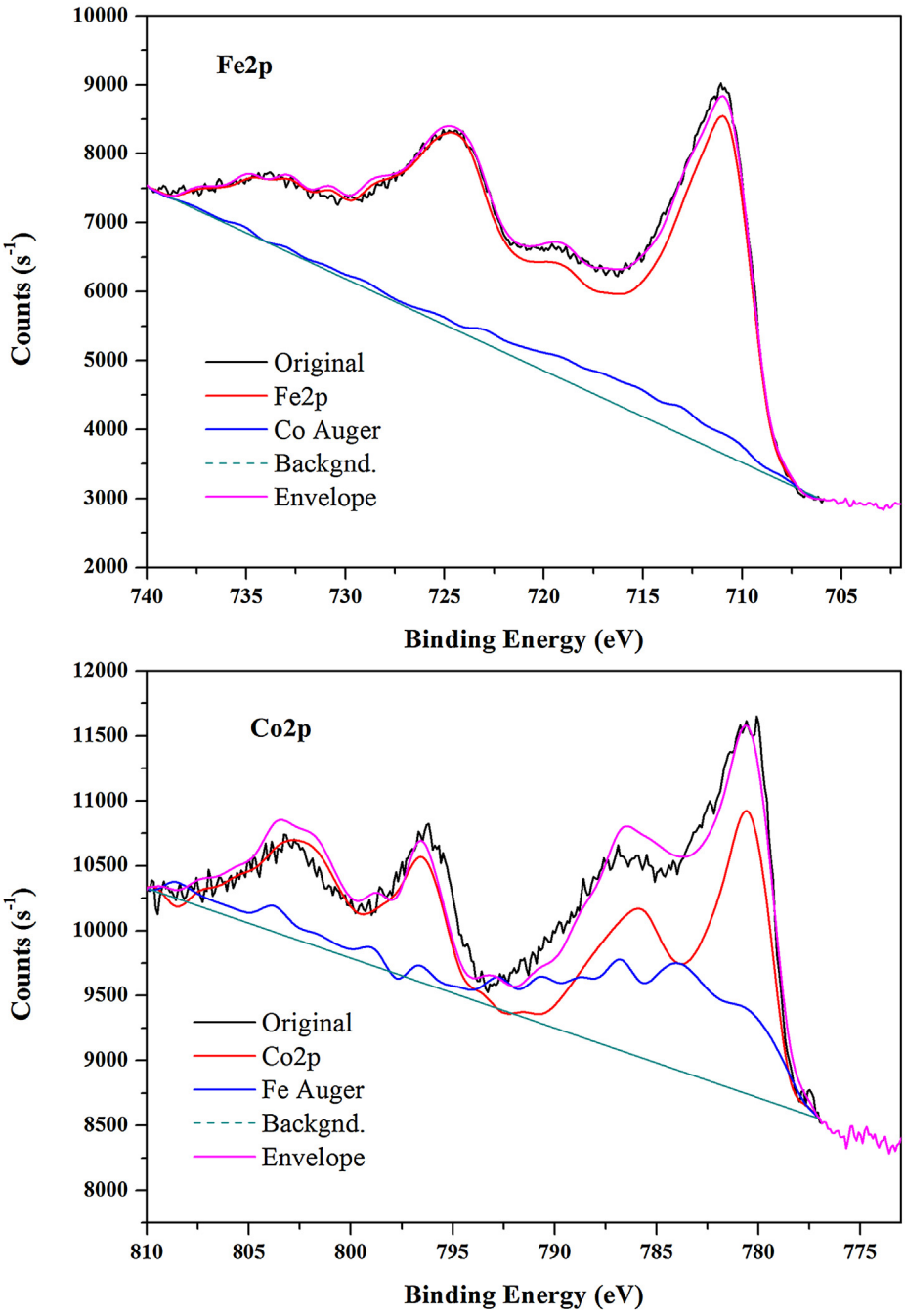

Fig. 5. NLLSF results for $S_{0.75}$.

amount, companied by the increase of Fe^{2+}/Fe^{3+} ratio, indicating the selective substitution of Fe^{3+} by cobalt.

The XRD patterns of prepared samples were similar to those of the standard card of magnetite (JCPDS: 19-0629) [22], indicating that all the introduction of Co cations did not clearly change the spinel structure of magnetite.

3.2. XPS analysis

3.2.1. Reference spectra

Fig. 1 presents the XPS survey curves for reference samples for the Fe 2p (magnetite) and Co 2p (cobalt chloride) regions. The C 1s peak in these two spectra and the O 1s signal in Fig. 1b were attributed to compounds adsorbed on the surfaces of the samples due to exposed to air. For magnetite, the peak positions of Fe $2p_{3/2}$ and Fe $2p_{1/2}$ were 710.8 and 724.1 eV, respectively. Each peak possessed a broadened satellite peak. The Co $2p_{3/2}$ and Co $2p_{1/2}$ peaks of cobalt chloride were observed at 781.1 and 797.1 eV, respectively. Obvious shake-up satellite features for Co $2p_{3/2}$ and Co $2p_{1/2}$ were also observed at 786.1 and 803.1 eV, respectively. The satellite peak at 786 eV is typically used to confirm the existence of divalent Co [23].

3.2.2. Original Fe 2p and Co 2p spectra

The original Fe2p and Co2p spectra of the Co-substituted magnetite samples are shown in Fig. 2. As the Co content increased, the peak intensities of Fe $2p_{3/2}$ (710.8 eV) and Fe $2p_{1/2}$ (724.1 eV) gradually weakened. The decrease in intensity was accompanied

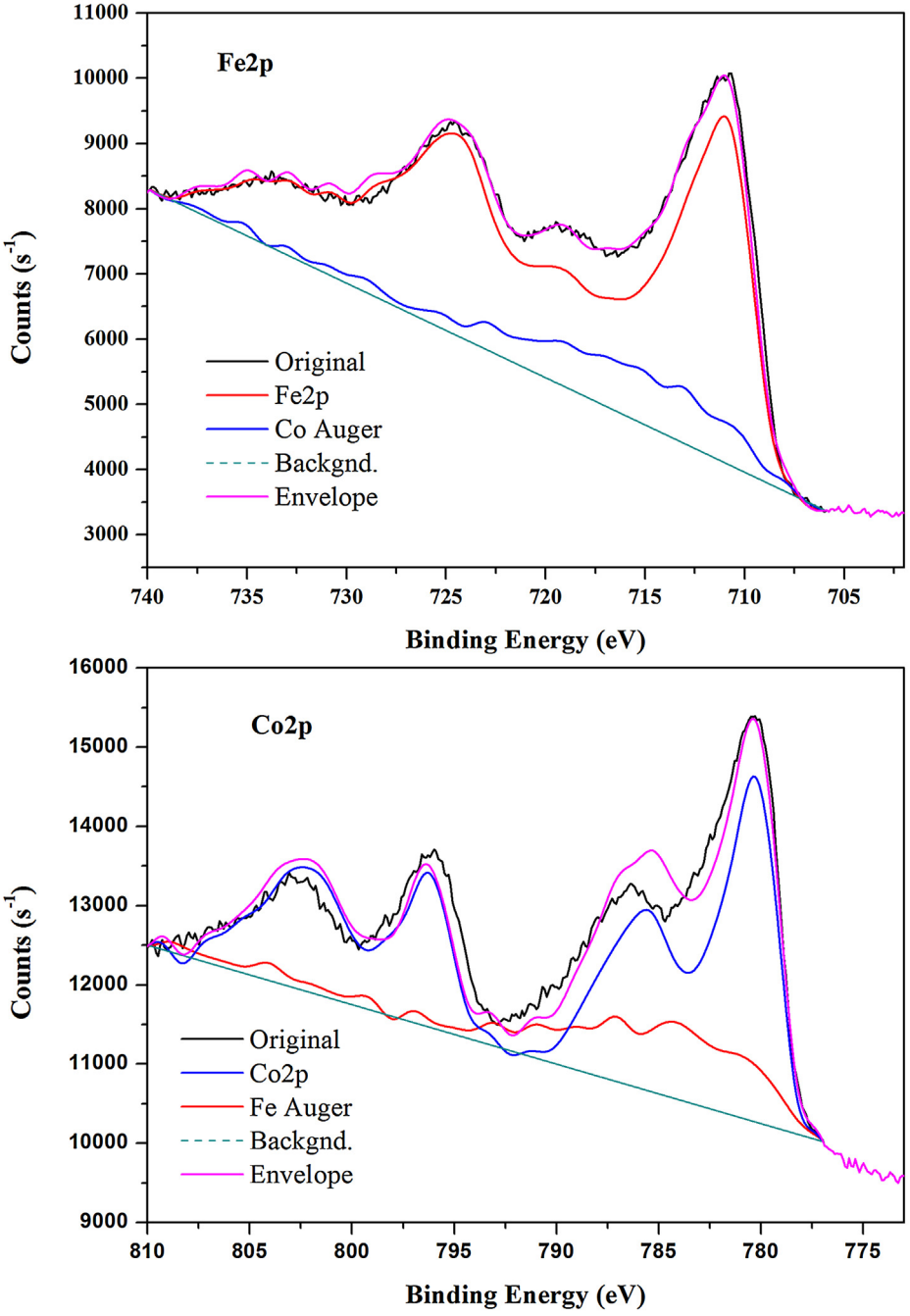

Fig. 6. NLLSF results for $S_{1.0}$.

by broadening of their peak shapes (Fig. 2a), indicating a decrease in Fe content in the samples and disturbance resulting from Co substitution. Simultaneously, the Co $2p_{3/2}$ and Co $2p_{1/2}$ peaks, and their satellite peaks became stronger and sharper with the increment of Co.

3.2.3. *NLLSF results for the original Fe 2p and Co 2p spectra*

Fig. 3 displays the NLLSF results for $S_{0.25}$. The Fe 2p spectrum derived from NLLSF coincided well with the original data and the envelope curve. The separated Auger peak of Co2p was very weak and nearly coincident with the background (Fig. 3a). Thus, at this a low doping amount (0.25), the overlapping effect of the Auger peak of Co2p on the XPS peak of Fe 2p can be ignored. Noise was clearly evident in the original Co2p spectrum, due to the very low content of Co in $S_{0.25}$ (Fig. 3b). Moreover, the coincidence of the original data and the obtained envelope curve for Co 2p after the fitting was not as strong as for Fe 2p, and the intensity of the Fe Auger peak was even stronger than the fitted XPS peak of Co 2p. Thus, there will be an error in the quantitative results of Co if the interference of Fe Auger peak is neglected.

As shown in Figs. 4, 5 and 6, with increasing Co, the match of the envelope curves of Co 2p obtained from NLLSF with the original Co 2p data improved. Furthermore, the fitted Co 2p peak became increasingly evident, whereas the peak intensity and peak area of the separated Fe Auger peak gradually decreased. When the Co doping amount was $\geq$0.50, the fitted peaks of Fe 2p started to deviate from the original data and the envelope curve due to the disturbance caused by Co Auger peak. Accordingly, a trend of con-

Table 2
Comparative data of Co/Fe atomic ratio in Co-substituted magnetite using different determination and fitting methods.

Sample	XPS				Chemical analysis
	method	Fe%	Co%	Co/Fe	Co/Fe
$S_{0.25}$	C	79.22	20.78	0.262	0.071
	N	93.72	6.28	0.067	
$S_{0.50}$	C	75.05	24.95	0.332	0.167
	N	87.15	12.85	0.147	
$S_{0.75}$	C	64.44	35.56	0.552	0.287
	N	77.15	22.85	0.296	
$S_{1.0}$	C	55.94	44.06	0.787	0.429
	N	64.57	35.43	0.549	

tinuous enhancement of the separated Co Auger peak spectrum was observed with increasing Co doping amount. Overall, the changes in the peak intensity and peak area of the Fe Auger were more apparent than those of the Co Auger peak, implying that the interference effect of Fe on the quantitative analysis of Co content is greater than that of Co on Fe.

3.2.4. Quantitative analysis

After isolating the interference Auger peaks by NLLSF, the fitted Fe 2p and Co 2p peaks were used to calculate the atomic% of Fe and Co, respectively. The quantitative analysis results are given in Table 2. C indicates the control group, in which the original spectra were directly used without fitting to calculate the atomic% of Fe and Co, and N represents the group in which the atomic% were calculated using the fitted spectra of Fe 2p and Co 2p after NLLSF processing. With increasing Co, the calculated Fe% in both group C and group N generally decreased, whereas the calculated Co% exhibited an increasing trend. However, for the same sample, the obtained value of Fe% was clearly higher in group N than in group C, and the value of Co% exhibited the opposite trend. These profiles led to significant differences in the ratio of Co/Fe for these two groups.

As revealed by X-ray absorption fine structure (XAFS) spectroscopy previously, the Co atoms are uniformly distributed in the spinel structure of magnetite [24,25], which means that the atomic% of Co and Fe on the surface of the sample is similar to that of the whole sample. Thus, the ratio of Co/Fe obtained from the XPS results should be similar to that acquired from the chemical analysis. In the present study, comparison of the Co/Fe ratios of group C and group N with the chemical analysis results revealed that the values for group N were significantly better match to the chemical analysis data (Table 2). These results confirm the effectiveness and accuracy of the NLLSF method for the XPS quantitative calculation of Fe and Co coexisting in a single material.

3.3. Catalytic performance

To investigate the effect of the incorporation of Co on the reactivity of magnetite, the samples were used as heterogeneous catalysts in the degradation of acid orange II (AOII) by oxone at neutral pH [25]. The AOII degradation were described by a pseudo-first-order kinetic equation (see Supplementary data, Fig. S2). The k_{app} values (apparent pseudo-first-order rate constant (min^{-1})) were 1.92×10^{-4}, 0.0286, 0.0337, 0.0996, and 0.127 min^{-1} for the systems catalyzed by Fe_3O_4, $S_{0.25}$, $S_{0.50}$, $S_{0.75}$, and $S_{1.0}$, respectively. A remarkable positive relationship was observed between the Co/Fe ratio and the k_{app}, which reflected that Co substitution improved the reactivity of magnetite and the catalytic activity obviously enhanced with the increase of Co substitution in magnetite.

4. Conclusion

In this study, NLLSF was used to calculate the relative contents of Co and Fe in Co-substituted magnetite samples with different Co doping concentrations. NLLSF separated the XPS peaks of Co 2p and Fe 2p from the Fe and Co Auger peaks, respectively. Significantly more accurate quantification results for Co and Fe were obtained after the interference from the Auger peaks was eliminated. A catalysis study confirmed that Co substitution improved the reactivity of magnetite, and this catalytic activity was greatly enhanced with the increase of Co substitution in magnetite. This study confirms the importance and accuracy of NLLSF in XPS quantitative calculation of Fe and Co coexisting in a single material.

Acknowledgments

This work was financially supported by the National Natural Science Foundation of China (Grant Nos. 41302026 and 41572032), and Youth Innovation Promotion Association CAS (Grant No. 2014324). This is a contribution (no. IS-2279) from GIGCAS.

Appendix A. Supplementary data

Supplementary data associated with this article can be found, in the online version, at http://dx.doi.org/10.1016/j.apsusc.2016.07.146.

References

[1] X.L. Liang, Z.S. He, Y.H. Zhong, W. Tan, H.P. He, P. Yuan, J.X. Zhu, J. Zhang, The effect of transition metal substitution on the catalytic activity of magnetite in heterogeneous Fenton reaction: in interfacial view, Colloids Surf. A 435 (2013) 28–35.
[2] R.C.C. Costa, M.d.F.F. Lelis, L.C.A. Oliveira, J.D. Fabris, J.D. Ardisson, R.R.V.A. Rios, C.N. Silva, R.M. Lago, Remarkable effect of Co and Mn on the activity of $Fe_{3-x}M_xO_4$ promoted oxidation of organic contaminants in aqueous medium with H_2O_2, Catal. Commun. 4 (2003) 525–529.
[3] R.C.C. Costa, M.F.F. Lelis, L.C.A. Oliveira, J.D. Fabris, J.D. Ardisson, R.R.V.A. Rios, C.N. Silva, R.M. Lago, Novel active heterogeneous Fenton system based on $Fe_{3-x}M_xO_4$ (Fe, Co, Mn, Ni): the role of M^{2+} species on the reactivity towards H_2O_2 reactions, J. Hazard. Mater. 129 (2006) 171–178.
[4] P. Liu, H.P. He, G.L. Wei, X.L. Liang, F.H. Qi, F.D. Tan, W. Tan, J.X. Zhu, R.L. Zhu, of Mn substitution on the promoted formaldehyde oxidation over spinel ferrite: catalyst characterization, performance and reaction mechanism, Appl. Catal. B-Environ. 182 (2016) 476–484.
[5] Y.H. Zhong, X.L. Liang, Z.S. He, W. Tan, J.X. Zhu, P. Yuan, R.L. Zhu, H.P. He, The constraints of transition metal substitutions (Ti, Cr, Mn, Co and Ni) in magnetite on its catalytic activity in heterogeneous Fenton and UV/Fenton reaction: from the perspective of hydroxyl radical generation, Appl. Catal. B-Environ. 150–151 (2014) 612–618.
[6] L.C.A. Oliveira, J.D. Fabris, R.R.V.A. Rios, W.N. Mussel, R.M. Lago, $Fe_{3-x}Mn_xO_4$ catalysts: phase transformations and carbon monoxide oxidation, Appl. Catal. A-Gen. 259 (2004) 253–259.
[7] X.L. Liang, S.Y. Zhu, Y.H. Zhong, J.X. Zhu, P. Yuan, H.P. He, J. Zhang, The remarkable effect of vanadium doping on the adsorption and catalytic activity of magnetite in the decolorization of methylene blue, Appl. Catal. B-Environ. 97 (2010) 151–159.
[8] C.G. Ramankutty, S. Sugunan, Surface properties and catalytic activity of ferrospinels of nickel cobalt and copper, prepared by soft chemical methods, Appl. Catal. A-Gen. 218 (2001) 39–51.
[9] N.H. Turner, J.A. Schreifels, Surface analysis: X-ray photoelectron spectroscopy and auger electron spectroscopy, Anal. Chem. 72 (2000) 99–110.
[10] A.P. Grosvenor, B.A. Kobe, M.C. Biesinger, N.S. McIntyre, Investigation of multiplet splitting of Fe 2p XPS spectra and bonding in iron compounds, Surf. Interface Anal. 36 (2004) 1564–1574.
[11] T. Yamashita, P. Hayes, Analysis of XPS spectra of Fe^{2+} and Fe^{3+} ions in oxide materials, Appl. Surf. Sci. 254 (2008) 2441–2449.
[12] S.E. Aamrani, J. Giménez, M. Rovira, F. Seco, M. Grivé, J. Bruno, L. Duro, J. de Pablo, A spectroscopic study of uranium(VI) interaction with magnetite, Appl. Surf. Sci. 253 (2007) 8794–8797.
[13] S.R. Chowdhury, E.K. Yanful, A.R. Pratt, Chemical states in XPS and Raman analysis during removal of Cr(VI) from contaminated water by mixed maghemite?magnetite nanoparticles, J. Hazard. Mater. 235–236 (2012) 246–256.
[14] Y. Jung, J. Choi, W. Lee, Spectroscopic investigation of magnetite surface for the reduction of hexavalent chromium, Chemosphere 68 (2007) 1968–1975.

[15] M.C. Biesinger, B.P. Payne, A.P. Grosvenor, L.W.M. Lau, A.R. Gerson, R.S.C. Smart, Resolving surface chemical states in XPS analysis of first row transition metals, oxides and hydroxides: Cr, Mn, Fe, Co and Ni, Appl. Surf. Sci. 257 (2011) 2717–2730.
[16] Handbook of X-ray Photoelectron Spectroscopy: a Reference Book of Standard Spectra for Identification and Interpretation of XPS Data, in: J.F. Moulder, J. Chastain, R.C. King (Eds.), Perkin-Elmer, Eden Prairie, MN, 1992.
[17] M. Aronniemi, J. Sainio, J. Lahtinen, Chemical state quantification of iron and chromium oxides using XPS: the effect of the background subtraction method, Surf. Sci. 578 (2005) 108–123.
[18] M. Oku, S. Suzuki, N. Ohtsu, T. Shishido, K. Wagatsuma, Comparison of intrinsic zero-energy loss and shirley-type background corrected profiles of XPS spectra for quantitative surface analysis: study of Cr, Mn and Fe oxides, Appl. Surf. Sci. 254 (2008) 5141–5148.
[19] K. Jitmanee, S.K. Hartwell, J. Jakmunee, S. Jayasvasti, J. Ruzicka, K. Grudpan, A simple flow injection system with bead injection for trace iron determination, Talanta 57 (2002) 187–192.
[20] T.S. Pasakarnis, M.I. Boyanov, K.M. Kemner, B. Mishra, E.J. O'Loughlin, G. Parkin, M.M. Scherer, Influence of chloride and Fe(II) content on the reduction of Hg(II) by magnetite, Environ. Sci. Technol. 47 (2013) 6987–6994.
[21] J. Ghasemi, N. Shahabadi, H.R. Seraji, Spectrophotometric simultaneous determination of cobalt, copper and nickel using nitroso-R-salt in alloys by partial least squares, Anal. Chim. Acta 510 (2004) 121–126.
[22] R. Zhao, K. Jia, J.-J. Wei, J.-X. Pu, X.-B. Liu, Hierarchically nanostructured Fe_3O_4 microspheres and their novel microwave electromagnetic properties, Mater. Lett. 64 (2010) 457–459.
[23] E.B. Castro, C.A. Gervasi, Electrodeposited Ni-Co-oxide electrodes:characterization and kinetics of the oxygen evolution reaction, Int. J. Hydrogen Energy 25 (2000) 1163–1170.
[24] X.L. Liang, Z.S. He, W. Tan, P. Liu, J.X. Zhu, J. Zhang, H.P. He, The oxidation state and microstructural environment of transition metals (V, Co, and Ni) in magnetite: an XAFS study, Phys. Chem. Miner. 42 (2015) 373–383.
[25] G.L. Wei, X.L. Liang, Z.S. He, Y.S. Liao, Z.Y. Xie, P. Liu, S.C. Ji, H.P. He, D.Q. Li, J. Zhang, Heterogeneous activation of Oxone by substituted magnetites $Fe_{3-x}M_xO_4$ (Cr, Mn Co, Ni) for degradation of Acid Orange II at neutral pH, J. Mol. Catal. A-Chem. 398 (2015) 86–94.